

Adsorption and Reactions of Tetraethoxysilane (TEOS) on Clean and Water-Dosed Titanium Dioxide (110)

L. Gamble,[†] M. B. Hugenschmidt,[†] C. T. Campbell,[†] Teresa A. Jurgens,[‡] and J. W. Rogers, Jr.^{*,‡}

Contribution from the Departments of Chemistry and Chemical Engineering, University of Washington, Seattle, Washington 98195

Received April 19, 1993[®]

Abstract: The adsorption and reactions of tetraethoxysilane (TEOS) vapor on clean and water-pretreated rutile TiO₂ (110) have been studied using temperature-programmed desorption (TPD), low-energy electron diffraction (LEED), and X-ray photoelectron spectroscopy (XPS). The molecule sticks with a probability near unity at temperatures of 130–300 K, and at low coverage, TEOS dissociates upon heating. At higher coverages, some desorbs. On the water- and hydroxyl-free surface, the dissociation reaction occurs rapidly between 200 and 350 K, with the initial products being Si(OEt)_{2,s} plus 2EtO_s (Et = C₂H₅). This is a new mechanism for silane coupling to oxide surfaces which requires neither hydroxyl groups nor surface defects. The EtO ligands, whether attached to Ti or Si atoms, decompose at ~650 K via β-hydrogen elimination to yield ethylene gas and surface-bound hydrogen, which rapidly attaches to another EtO ligand, yielding ethanol gas. By 700 K, the net products evolved are equal amounts of ethylene and ethanol gas (two molecules of each per dissociated TEOS molecule), while SiO₂ remains on the surface. With pretreated D₂O, the initial reaction also leads to Si(OEt)_{2,s} + 2EtO_s, but the EtO_s thus produced now reacts with the D₂O_s and/or OD_s to give an EtOD peak in the TPD spectrum at ~350 K. The amount of TEOS which dissociates is nearly doubled when D₂O is present in high coverages. This is attributed to the fact that the D₂O enhances elimination of EtO_s (as EtOD), thus creating more free sites to accommodate dissociation products. The Si(OEt)_{2,s} species is much less reactive with water than EtO_s and will remain on the surface to 600 K in TPD, irrespective of water pretreatment.

Introduction

Organofunctional silanes are frequently used as coupling or bonding agents between dissimilar phases. Silane coupling agents are often of the form RSiX₃, where X represents a halide, alkoxide, or alkyl group that can react with the surface and R represents an organofunctionality.^{1,2} By carefully selecting the R group, silane coupling agents can be used for protective layer coatings, electronic sensors, chemically modified electrodes, thin film optics,³ and antireflection coatings.^{4,5} Recently, advances in the microelectronics industry have stimulated the use of alkoxysilanes as gaseous precursors for the growth of SiO₂ dielectric layers⁶ by chemical vapor deposition (CVD). In addition to incorporating Si and O in a single source molecule, alkoxysilanes are less hazardous than traditional vapor-phase silicon sources, such as silanes and chlorosilanes.⁶ Furthermore, dielectric layers deposited from alkoxysilane precursors allow deposition of doped silica layers, high growth rates, and conformal step coverage.⁷ For applications involving deposition of SiO₂ films, the precursor of choice has been tetraethoxysilane, or TEOS.⁶⁻¹⁰

In this paper, we examine the fundamental surface processes important to the adsorption and reaction of gaseous TEOS on a TiO₂(110) single-crystal surface in an ultra-high-vacuum surface analysis chamber, including reaction products as a function of

temperature and surface water (D₂O) concentration. Ultimately, a detailed understanding of these deposition/adsorption characteristics, reaction mechanisms, and reaction intermediates is necessary in order to grow better SiO₂ films on TiO₂ and to develop better silane coupling chemistry for functionalizing TiO₂ surfaces. We show here that silane coupling to TiO₂, forming Ti–O–Si bonds, occurs with high probability below 350 K, even in the absence of surface hydroxyl sites. The classical mechanism of silane coupling to oxides requires surface hydroxyl sites.¹

Relatively few studies have reported using TEOS to produce thin films *in vacuo*.^{5,10-15} The adsorption and decomposition of TEOS was studied previously on clean Si(100) and amorphous, hydroxylated SiO₂.^{6,16} TEOS was found to react with either surface at 450 K to produce an intermediate mixture of adsorbed di- and triethoxysilanes.¹⁶ Upon heating in vacuum these intermediates decomposed to evolve ethylene and hydrogen or water. Crowell *et al.* found three distinct TPD peaks for ethylene, centered at 500, 600, and 720 K.¹⁶ In related studies, ethanol adsorption on SiO₂ was shown to model the chemistry of TEOS on SiO₂,¹¹ with ethanol exposures at 450 K leading to the formation of ethoxide species bound to surface silicon. Exposure of alkoxy silanes to severely dehydroxylated SiO₂ gave silane-coupling reactions both at the remaining surface hydroxyl groups and at strained Si–O–Si defects.^{12,14,15} On clean MgO(100), trimethoxysilane was shown to eliminate methoxy and form Si–O–Mg bonds to the surface in the absence of surface hydroxyls.¹³ To our knowledge, no prior studies have examined the reactions of TEOS on any well-ordered single crystal as a detailed function of water (D₂O) preexposure, as we do here.

Our previous study¹⁷ of water adsorption on this TiO₂(110) surface serves as important background for this study. There,

[†] Department of Chemistry.

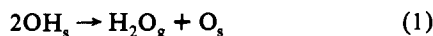
[‡] Department of Chemical Engineering.

[®] Abstract published in *Advance ACS Abstracts*, November 1, 1993.

- (1) Plueddemann, E. P. *Silane Coupling Agents*; Plenum: New York, 1982.
- (2) Brinker, C. J.; Scherer, G. W. *Sol-Gel Science: The Physics and Chemistry of Sol-Gel Processing*; Academic Press: New York, 1990 p 1.
- (3) Kurth, D. G.; Bein, T. *J. Phys. Chem.* **1992**, *96*, 6707.
- (4) Okuhara, T.; White, J. M. *Appl. Surf. Sci.* **1987**, *29*, 223.
- (5) Brinker, C. J.; Harrington, M. S. *Sol. Energy Mat.* **1981**, *5*, 159.
- (6) Crowell, J. E.; Tedder, L. L.; Cho, H.-C.; Cascarano, F. M.; Logan, M. A. *J. Vac. Sci. Technol. A* **1990**, *8*, 1864.
- (7) Becker, F. S.; Pawlik, D.; Anzinger, H.; Spitzer, A. *J. Vac. Sci. Technol. B* **1987**, *5*, 1555.
- (8) Levy, R. A.; Gallagher, P. K.; Schrey, F. *J. Electrochem. Soc.* **1987**, *134*, 430.
- (9) Adams, A. C.; Capio, C. D. *J. Electrochem. Soc.* **1979**, *126*, 1042.
- (10) Jin, T.; Jo, S. K.; Yoon, C.; White, J. M. *Chem. Mat.* **1989**, *1*, 308.

- (11) Tedder, L. L.; Lu, G.; Crowell, J. E. *J. Appl. Phys.* **1991**, *69*, 7037.
- (12) Tedder, L. L.; Crowell, J. E.; Logan, M. A. *J. Vac. Sci. Technol. A* **1991**, *9*, 1002.
- (13) Danner, J. B.; Vohs, J. M. *Appl. Surf. Sci.* **1992**, *62*, 255.
- (14) Dubois, L. H.; Zegarski, B. R. *J. Am. Chem. Soc.* **1993**, *115*, 1190.
- (15) Dubois, L. H.; Zegarski, B. R. *J. Phys. Chem.* **1993**, *97*, 1665.
- (16) Crowell, J. E.; Tedder, L. L.; Cho, H. C.; Cascarano, F. M.; Logan, M. A. *J. Electron Spectrosc. Relat. Phenom.* **1990**, *54/55*, 1097.

we found that water adsorbs mainly molecularly on this nearly stoichiometric surface at 110 K. The maximum water coverage before formation of multilayer-like water TPD peaks was ~ 1.0 water molecule per $\text{TiO}_2(110)$ unit cell, attributed to one molecule bound at each Ti^{4+} site.¹⁷ We will refer to this coverage as a "monolayer of H_2O " below. Upon heating, this water desorbs molecularly in a peak at ~ 260 K. A tail of this water TPD peak to ~ 350 K was attributed to the low coverages (~ 0.1 – 0.25 monolayer) of hydroxyl groups reported previously^{18–20} which disproportionates at 300–350 K via the reaction



Here the subscript "s" refers to a surface species bound to TiO_2 , and "g" refers to gaseous. A 170 K water TPD peak, which populates at higher coverages, is attributed to water bound at oxygen anion sites, but since it is unresolved from the 160 K peak for water multilayers,¹⁷ we will refer here to these two states collectively as "multilayer water".

Experimental Section

Experiments were performed in an ultra-high-vacuum (UHV) system, consisting of two chambers: a preparation chamber and an analytical chamber. The details of the apparatus are presented in a previous paper.²¹ TEOS dosing and LEED were performed in the preparation chamber, while TPD and XPS data were taken in the analytical chamber. The two chambers were connected via a stainless-steel rod on which the sample was mounted for heating, cooling, translation, and rotation. This allowed transfer of the sample from the preparation chamber to the analytical chamber after dosing, always maintaining temperature control. Typical base pressures in the preparation and analytical chambers were mid- and low- 10^{-10} Torr, respectively.

The polished rutile crystal substrate was obtained from Atomergic Chemetals Corporation and had the following dimensions: 10 mm long by 5 mm wide by 1 mm thick. The polished surface was oriented to within 0.5° of the (110) plane. The crystal was mounted on a tantalum support with a thin layer of indium between the support and the crystal to provide good electrical/thermal contact. By resistive heating or cooling of the tantalum support with liquid nitrogen, the sample temperature could easily be maintained between ~ 100 and 800 K. Temperatures were measured by a chromel–alumel thermocouple attached to the tantalum support. Prior to each set of experiments, the substrate was sputtered for 15 minutes at several microamperes Ar^+ current ($E_p = 500$ – 750 eV), followed by a brief 800 K anneal in 1 – 2×10^{-6} Torr of oxygen. The spectral line shape of the $\text{Ti}(2p)$ region was used as a diagnostic for the presence of defects on the surface. Distinct and well-resolved $\text{Ti}(2p_{1/2})$ and $\text{Ti}(2p_{3/2})$ peaks were observed from a defect-free surface, while surface defects, such as missing oxygen atoms, can be seen by changes in the XPS^{22,23} and AES line shapes.²⁴ Our cleaning treatment produced a well-ordered TiO_2 surface demonstrating a sharp $p(1 \times 1)$ LEED pattern²⁵ and the XPS line shapes and binding energies characteristic of stoichiometric TiO_2 .^{22,23,26} However, the oxidation was not so severe as to completely remove *bulk* oxygen vacancies which remained in a concentration sufficient to minimize charging effects during XPS experiments. Later atomic force microscopy (AFM) measurements on this sample indicate it had $<3\%$ surface defects.¹⁷

High-purity tetraethoxysilane (TEOS), distilled in quartz, was obtained from Petrarch Systems and was transferred under a nitrogen atmosphere to a glass vial which was connected to the UHV system. TEOS was

(17) Hugenschmidt, M. B.; Gamble, L.; Campbell, C. T. *Surf. Sci.*, in press.

(18) Kurtz, R. L.; Stockbauer, R.; Madey, T. E.; Roman, E.; De Segovia, J. L. *Surf. Sci.* **1989**, *218*, 178.

(19) Pan, J. M.; Maschhoff, B. L.; Diebold, U.; Madey, T. E. *J. Vac. Sci. Technol. A* **1992**, *10*, 2470.

(20) Thiel, P. A.; Madey, T. E. *Surf. Sci. Reports* **1987**, *7*, 211.

(21) Campbell, J. M.; Seimanides, S. G.; Campbell, C. T. *J. Phys. Chem.* **1989**, *93*, 815.

(22) Platau, A.; Johansson, L. I.; Hagstrom, A. L.; Karlsson, S. E.; Hagstrom, S. B. M. *Surf. Sci.* **1977**, *63*, 153.

(23) Ramqvist, L.; Hamrin, K.; Johansson, G.; Fahlman, A.; Nordling, C. *J. Phys. Chem. Solids* **1969**, *30*, 1835.

(24) Chung, Y. W.; Lo, W. J.; Somorjai, G. A. *Surf. Sci.* **1977**, *64*, 588.

(25) Henrich, V. E. *Prog. Surf. Sci.* **1979**, *9*, 143.

(26) Muilenberg, G. E., Ed., *Handbook of X-ray Photoelectron Spectroscopy*; Perkin-Elmer Corp.: Eden Prairie, MN, 1979; p 42.

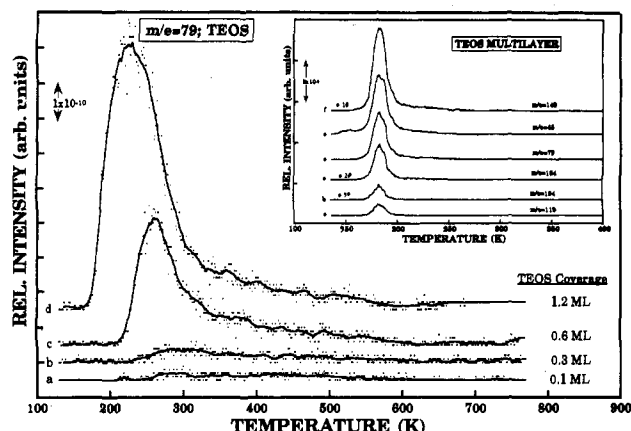


Figure 1. TPD spectra of molecular TEOS ($m/e = 79$) from a $\text{TiO}_2(110)$ surface with the indicated coverages of TEOS. Exposures were at ~ 130 K with no predosed water (D_2O). The inset shows the TPD spectra of representative TEOS mass fragments (a) $m/e = 119$, (b) $m/e = 194$, (c) $m/e = 164$, (d) $m/e = 79$, (e) $m/e = 45$, and (f) $m/e = 149$ from a multilayer (~ 15 ML) of TEOS on TiO_2 .

further purified by several freeze–pump–thaw cycles and was dosed to the substrate using helium as a carrier gas. D_2O , with a purity of 99.9% deuterium, was obtained from Cambridge Isotope Laboratories and was dosed through a normal leak valve after several freeze–pump–thaw cycles.

TEOS dosing and the oxygen anneal procedure described above were performed in the preparation chamber. The TEOS doser consisted of a straight, open-ended copper tube with an inside diameter of 5.25 mm, which was mounted on the 70 mm diameter Conflat flange of a leak valve. The length of the dosing tube was approximately 25 cm, or about 50 times the inner diameter of the tube, thus ensuring a sharp flux distribution directed at the surface,²⁷ which was a few millimeters from the end of the tube. Gaseous TEOS was mixed with helium in a TEOS/He ratio of 1:3 in a continuously pumped manifold attached to the high-pressure side of the leak valve. This had the advantages outlined previously.²⁸ Doses were measured by an ion gauge mounted inside the preparation chamber, which was sensitive primarily to the He carrier gas and gave a signal proportional to the TEOS flux on the sample. The standard dosing procedure included preconditioning the doser with a high flux of TEOS at the beginning of each set of experiments in order to passivate the dosing line and to reduce any undesirable reactions with the tube walls. The doser flux was calibrated against the traditional dosing method (backfilling) by comparing TPD peak areas. Experiments performed "in excess H_2O " described below were accomplished by removing the liquid nitrogen trap (for H_2O impurities) from the He carrier gas line.

TPD experiments used a quadrupole mass spectrometer (QMS—Inficon Quadrex 200) interfaced with an IBM PC. A typical TPD experiment consisted of pretreating the TiO_2 surface (which could include dosing a given quantity of D_2O or H_2O), followed by dosing TEOS to the sample in the preparation chamber. The sample was then transferred to the analytical chamber, positioned in front of the QMS, and heated for TPD at a rate of 4.5 K/s, following up to six masses.

XPS spectra were taken at 110 K with normal detection using a Leybold–Heraeus (LH-10) hemispherical electron energy analyzer operated at a pass energy of 100 eV and an $\text{Al}(K_{\alpha})$ X-ray source, which gave a working instrument resolution (fwhm) of ~ 1.7 eV. Binding energies (BEs) were reproducible to ± 0.1 eV, and the spectrometer was calibrated to the Fermi energy of gold [$\text{Au}(4f)_{7/2} = 84.0$ eV]. Using this calibration, the $\text{Ti}(2p_{3/2})$ peak for the clean, defect-free $\text{TiO}_2(110)$ crystal occurred at a BE of 458.8 eV, in excellent agreement with previously reported values.^{22,23}

Results

TPD of TEOS on $\text{TiO}_2(110)$ with no D_2O Predose. Figure 1 illustrates the TPD resulting from increasing exposures of TEOS to the $\text{TiO}_2(110)$ surface held at ~ 130 K. Curves a–d show the mass fragment $m/e = 79$, which is characteristic of molecular

(27) Campbell, C. T.; Valone, S. M. *J. Vac. Sci. Technol. A* **1985**, *3*, 408.

(28) Henn, F. C.; Bussell, M. E.; Campbell, C. T. *J. Vac. Sci. Relat. Phenom.* **1991**, *A9*, 10.

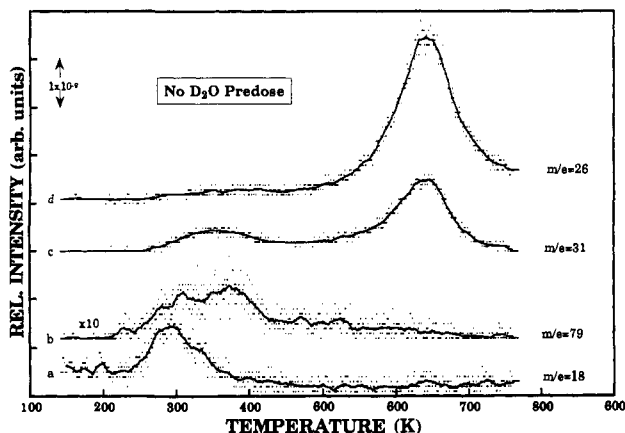


Figure 2. TPD spectra showing reaction products of TEOS on TiO_2 (110). TEOS was dosed to a surface held at ~ 130 K which had not been predosed with water or D_2O . Desorption products indicated are from (a) H_2O , $m/e = 18$; (b) TEOS, $m/e = 79$; (c) ethanol, $m/e = 31$; and (d) ethylene, $m/e = 26$.

desorption of TEOS. Curves a–c are for submonolayer coverages and exhibit a broad desorption feature extending over the range 220–450 K. At higher exposures (curve d), the first molecular layer saturates and is characterized by a TPD peak maximum at 230 K with a long tail extending to ~ 450 K. The presence and intensity of this tail depends upon the coverage of coadsorbed water impurity as we will show below. In the experiments of Figure 1, there was a sizable water impurity, and this tail is consequently of low intensity. Very high exposures lead to multilayer formation (inset) with the peak desorption temperature occurring at ~ 185 K. We define a monolayer (ML) as the coverage at which this first molecular layer saturates, prior to multilayer formation, as judged from the TPD line shape.

The inset of Figure 1 shows several of the mass fragments from the cracking pattern of TEOS which result from desorption of a thick TEOS multilayer (~ 15 ML). Characteristic mass fragments at $m/e = 45$, $m/e = 79$, $m/e = 119$, $m/e = 149$, $m/e = 164$, and $m/e = 194$ are shown, and all exhibit the same TPD line shape; other masses expected to have high intensities for TEOS ($m/e = 26$, 29, etc.) were followed in similar experiments and had similar spectra of appropriate intensity. Following desorption of the TEOS multilayer, the molecular peak desorbs beginning at 220 K, which appears as a broad tail on the larger multilayer peak. The small feature at ~ 145 K in the $m/e = 45$ spectrum (curve e of the inset) is due to desorption of molecular ethanol, which was an impurity in the TEOS source.

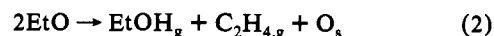
Not obvious from the masses displayed in Figure 1 is the fact that a reaction between TEOS and the TiO_2 surface also occurs which evolves ethanol and ethylene at higher temperatures. This reaction is dependent on the presence or absence of H_2O , or OH_x (or in the case of deuterium labeling, D_2O , or OD_x). This reaction was investigated in detail, and we will later present TPD spectra for submonolayer doses of TEOS as a function of water predose.

Figure 2 illustrates the desorption spectra from a TiO_2 surface exposed to TEOS at ~ 130 K where every effort was made to minimize the water impurity. The resulting TEOS coverage is ~ 0.3 ML. The TPD spectra in curves a–d show characteristic mass fragments from water ($m/e = 18$), TEOS ($m/e = 79$), ethanol ($m/e = 31$), and ethylene ($m/e = 26$), respectively. Water desorbs in its usual temperature range (250–350 K) for low coverage, with a peak maximum near 300 K.¹⁷ This feature results from a small and unavoidable amount of H_2O impurity. The intensity of this peak above 300 K has been attributed to hydroxyl disproportionation (reaction 1 above),^{17,18} where the reverse reaction led to OH_x . The unresolved intensity below 300 K is due to molecular water desorption.¹⁷

As discussed with Figure 1, TEOS desorbs over a broad temperature range from 220 to 450 K (curve b). The desorption of ethylene ($m/e = 26$) is shown in curve d, where a high-temperature desorption peak, centered at about 650 K, is observed. Hereafter, we will refer to reaction products desorbing at 650 K as the “high-temperature desorption peak”. The TPD spectrum for ethanol, $m/e = 31$, is illustrated in curve c. Ethanol desorbs simultaneously with ethylene in the high-temperature desorption peak. In addition, a low temperature desorption peak is observed for ethanol at about 350 K. This desorption peak is coupled to the presence of the water/hydroxyl impurity on the surface and will be addressed below where D_2O was predosed. The only other desorption product of any significance detected during the TPD experiments was diethyl ether, which desorbed in very low concentration over the temperature range 450–770 K.

Ethanol was monitored by $m/e = 31$ rather than $m/e = 45$ or 46 because the former mass was a component of the TEOS molecular cracking pattern (see the inset of Figure 1) and the latter mass was much weaker in intensity. However, we did verify that the TPD peaks assigned to ethanol did have the proper intensities at $m/e = 45$ and 46 and other masses, such as $m/e = 29$ and 27, expected for ethanol. For similar reasons, ethylene was monitored by $m/e = 26$ rather than $m/e = 28$, which had contributions from other desorbing species and background gases in the chamber. During ethylene desorption, other mass fragments expected for ethylene such as $m/e = 28$, 27, and 25 were monitored to verify they had the proper intensities.^{29,30} Ethanol has a significant cracking fragment at $m/e = 26$, which was accounted for in quantifying ethylene signals when both were simultaneously desorbed. In addition, the transmission of this QMS decreases strongly with increasing mass. For these reasons, fragmentation and sensitivity calibrations were performed on this QMS for ethanol and ethylene. These measurements showed that the spectrometer is ~ 2.2 times as sensitive to ethylene at $m/e = 26$ as it is to ethanol at $m/e = 31$. Using this calibration, the peak areas for the high-temperature desorption peak suggest an ethylene/ethanol molar ratio of 1:1. This ratio did not vary with surface water coverage (discussed below), magnitude of TEOS dose, or temperature of TEOS dose between 130 and 300 K.

The 1:1 ratio suggests a β -hydrogen elimination mechanism involving dehydrogenation of an ethoxy group, which desorbs as ethylene, followed by rapid transfer of the hydrogen to a neighboring ethoxy group which desorbs as ethanol, and leaving one oxygen bound to the surface:



With ethoxy groups adsorbed on {110}-faceted rutile $\text{TiO}_2(001)$, this same process is known to occur at the same temperature of 650 K and with the same product ratio.³¹ Similar β -hydrogen elimination reactions (but with different product distributions) occur at 650 K for ethoxy bound to TiO_2 (anatase) powder³² and $\text{Si}(100)$ ⁶ and at 600 K for ethoxy bound to SiO_2 powder.⁶ The similarity of these desorption temperatures suggests the same process is occurring here. However, we cannot yet tell whether the ethoxy groups involved in the β -hydrogen elimination are bound to Ti or Si atoms, or to both. This point will be addressed below.

TPD of TEOS on $\text{TiO}_2(110)$ with Varying D_2O Predose. Adsorption and decomposition of TEOS on TiO_2 was also studied with varying D_2O predoses. The exposure series shown in Figure 3A–E illustrates the desorption spectra for TEOS, its decomposition products, and D_2O as a function of increasing D_2O precoverage. For each figure, the clean TiO_2 crystal was exposed

(29) *Eight Peak Index of Mass Spectra*, 3rd ed.; The Royal Society of Chemistry: Herts, U.K., 1983, p 1.

(30) McLafferty, F. W.; Stauffer, D. B. *The Wiley/NBS Registry of Mass Spectral Data*; Wiley-Interscience: New York, 1989; p 1.

(31) Kim, K. S.; Barteau, M. A. *J. Molec. Catal.* **1990**, *63*, 103.

(32) Kim, K. S.; Barteau, M. A.; Farneth, W. E. *Langmuir* **1988**, *4*, 533.

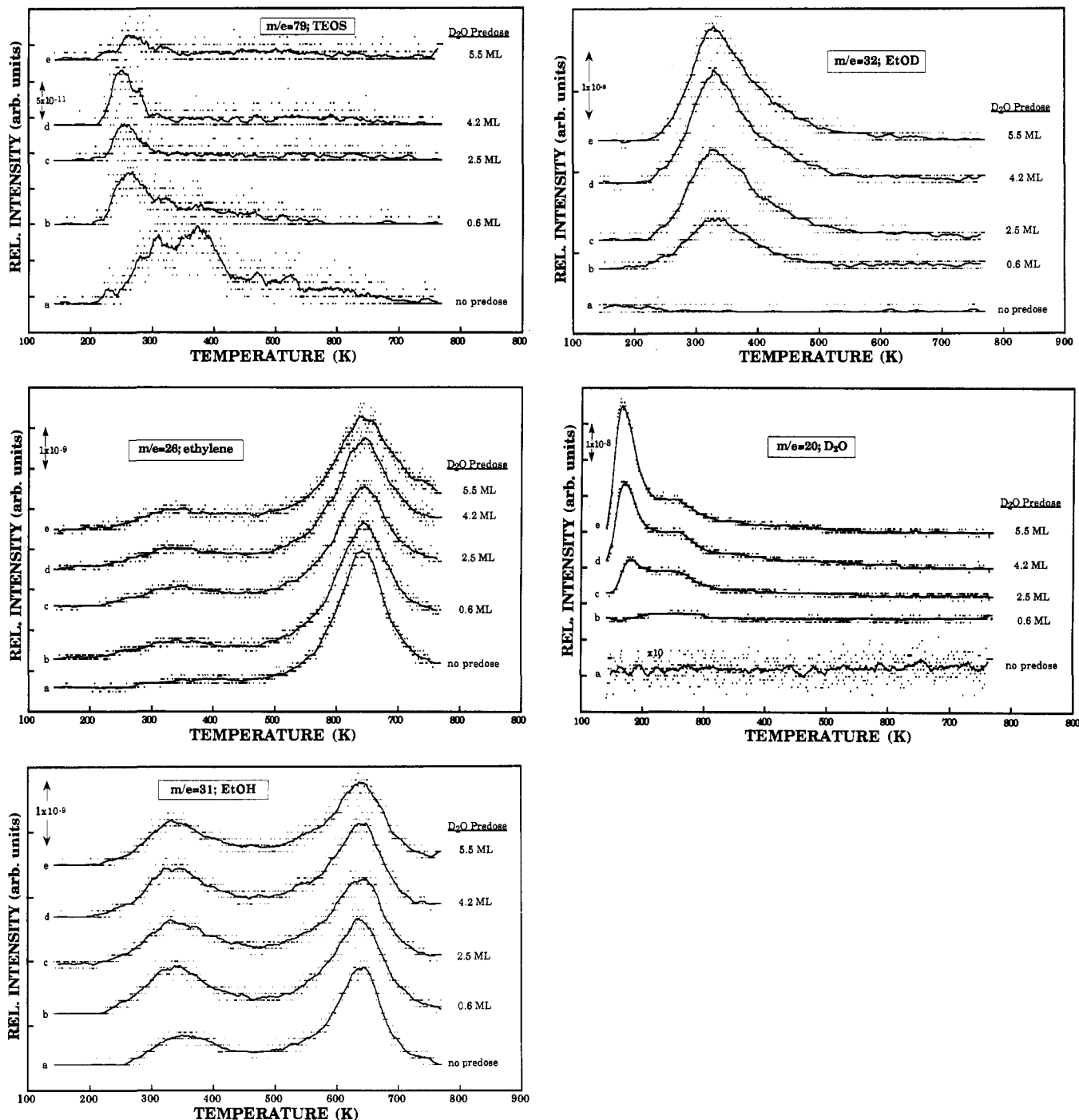


Figure 3. TPD spectra for (A) TEOS, $m/e = 79$; (B) ethylene, $m/e = 26$; (C) EtOH, $m/e = 31$; (D) EtOD, $m/e = 32$; and (E) D_2O , $m/e = 20$ as a function of D_2O predose. $TiO_2(110)$ at 130 K was exposed to the indicated precoverage of D_2O , followed by a standard exposure of TEOS to give ~ 0.3 ML coverage. D_2O precoverages were (a) no predose (0.2 ML of H_2O from background adsorption), (b) 0.6 ML, (c) 2.5 ML, (d) 4.2 ML, and (e) 5.5 ML. Large amounts of HDO and H_2O were included in the " D_2O predose" (see text).

to the same amount of TEOS, which led to a coverage of ~ 0.3 ML, following the indicated D_2O predose. About 50% of the deuterium in the D_2O exchanged with hydrogen on the doser and chamber walls prior to predosing, such that HDO and H_2O were also predosed. The " D_2O predose" coverages reported in the figure are the equivalent MLs of total water ($D_2O + HDO + H_2O$) desorbed.

The TPD of molecular TEOS ($m/e = 79$) as a function of D_2O predose is shown in Figure 3A. Curve a shows the TPD with no D_2O predose. As was observed in Figure 2 (curve b), the TEOS desorbs over a broad temperature range from 220 to 450 K with no well-resolved peaks. As the D_2O precoverage is increased (curves b–e), the intensity and area of the TPD peaks drop

precipitously, particularly at temperatures above 300 K. The overall line shape narrows as the desorption intensity above 300 K decreases. At higher D_2O precoverage, the TPD line shape changes to a single, well-resolved feature centered at ~ 260 K whose area continues to decrease as the D_2O precoverage increases. Because the TEOS exposures were the same for each curve in the figure, this behavior of the molecular TEOS TPD peaks suggests that the amount of TEOS which dissociates to form surface-bound products increases as the D_2O precoverage increases. This trend is consistent with the behavior of the desorption of TEOS dissociation products presented below. The activation energy for desorption of TEOS at low water coverage can be estimated

from a simple Redhead analysis³³ of the peak temperature, T_p , in the TPD spectra. Assuming a preexponential factor of 10^{13} s⁻¹ for desorption,³⁴ the activation energy for $T_p \approx 275$ K is 16.6 ± 0.5 kcal/mol. States of lower activation energy are populated at higher TEOS coverage (see Figure 1).

The resulting TPD curves for $m/e = 26$, which is predominantly due to ethylene, are in Figure 3B. For the high-temperature peak in curves a–e, the desorption temperature remains constant but the line shape broadens and the maximum peak intensity and peak area decrease slightly with increasing D₂O precoverage. The broad desorption features centered near 350 K in curves b–e are contributions to the $m/e = 26$ signal from ethanol desorption.

In contrast to the case of the single desorption peak observed for ethylene, ethanol desorbs in two distinct peaks as illustrated in Figure 3C, which shows the corresponding TPD spectra for $m/e = 31$. The high-temperature desorption peak is centered at ~ 650 K simultaneous with the ethylene peak, and a low-temperature peak is centered at ~ 350 K. As shown in curves a–e, the desorption temperature of the high-temperature peak is independent of the D₂O precoverage, but the peak shape broadens and the peak area decreases slightly with increasing D₂O precoverage. Independent of D₂O precoverage, the areas of the high-temperature desorption peaks for ethanol and ethylene indicate that the two species still desorb in a 1:1 ratio.

Interaction of TEOS with impurity H₂O_s (or OH_s), dosed along with the D₂O, is responsible for the EtOH desorbed in the low-temperature peak; the mechanism is discussed below. The low-temperature EtOH peak grows slightly with D₂O (plus HDO) precoverage. Note that in the "no D₂O precoverage" experiment (curve a), a small amount of H₂O is still dosed to the cold TiO₂ surface along with the TEOS. (Figure 2 contains the same data for the "no D₂O precoverage" experiments that is shown in Figure 3.) Desorption of this H₂O ($m/e = 18$) is shown in curve a of Figure 2.

Figure 3D illustrates the corresponding TPD spectra for $m/e = 32$, which is mainly due to EtOD. As expected, no EtOD desorption is observed in the absence of predosed D₂O (curve a). However, as the precoverage of D₂O is increased from 0.6 to 5.5 ML, an intense EtOD desorption peak at 350 K develops whose magnitude increases monotonically with increasing D₂O precoverage (curves b–e). This peak is simultaneous with the EtOH peak at 350 K. Since surface ethoxy groups on TiO₂(110) facets are known to react with surface OH to produce EtOH in a TPD peak at 350 K,³¹ we propose that this 350 K peak for EtOH and EtOD is also due to this reaction of EtO groups bound to Ti sites of the (110) surface. No high-temperature desorption peak is observed for EtOD.

Finally, the corresponding TPD spectra for D₂O ($m/e = 20$) are shown in Figure 3E. For low coverages of D₂O, a low intensity, broad desorption feature is observed in the range 200–300 K. This is close to the usual desorption temperature (230–300 K) for molecularly adsorbed water on Ti⁴⁺ sites on this surface.¹⁷ As the D₂O coverage is increased to greater than a monolayer (curves c–e), this feature saturates and the multilayer water desorption peak (also due to anion sites¹⁷) is observed at its usual temperature of 170 K.¹⁷ The presence of ~ 0.1 – 0.25 ML of OD_s, which gives rise to desorption intensity between 300 and 350 K,¹⁷ is also expected after D₂O predoses.¹⁷ The TPD spectra in curves b–e indeed show a weak tail extending to ~ 350 K attributable to such hydroxyl disproportionation. Its intensity may be low here due to the additional consumption of hydroxyls by reaction with EtO_s. Not shown are the $m/e = 18$ and $m/e = 19$ spectra for the same exposure series; these spectra were very similar to those observed for $m/e = 20$, except for the extra intensity of $m/e = 18$ with no D₂O precoverage (Figure 2, curve a). The peak areas of these features indicated D₂O/HDO/H₂O ratios of $\sim 1:1:1$.

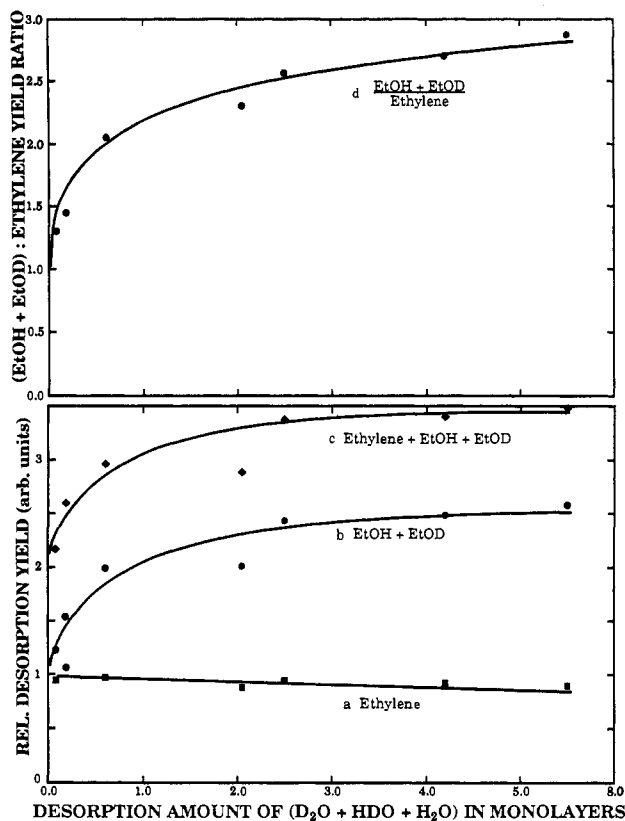


Figure 4. Relative desorption yield of carbon-containing products as a function of water precoverage. (a) ■ ethylene, $m/e = 26$; (b) ● EtOH + EtOD, $m/e = 32 + 31$; and (c) ◆ ethylene + EtOD + EtOH, $m/e = 26 + 32 + 31$. (d) The (EtOD + EtOH) to ethylene yield ratio as a function of preadsorbed water. The abscissa is MLs of desorbed water.

(The D content increased with the size of the water precoverage, so this is only an average ratio.)

After desorption of molecular TEOS, the only carbon-containing species observed to desorb in large quantities are ethanol and ethylene. The amount of ethylene and ethanol which desorbs from the surface during TPD can be determined from the areas under their peaks. Below, we will show XPS evidence that all carbon is desorbed from the surface by 770 K. Thus we can follow the extent of the TEOS reaction with TiO₂ as a function of surface water by monitoring the ethylene, ethanol, and water TPD peak areas. This analysis, for the water-predosing experiments from Figure 3A–E, is summarized in Figure 4 where the peak areas for the desorbed TEOS decomposition products (EtOH, EtOD, and ethylene) are plotted as a function of the total water TPD peak area (D₂O + DHO + H₂O). The peak areas for the desorption products were corrected for cracking patterns and QMS sensitivities.

Curve a shows the ethylene desorption as a function of water precoverage; ethylene desorption decreases slightly as the water precoverage is increased. In contrast, the amount of total ethanol desorption (curve b) doubles as the water precoverage increases, compared to the extrapolated zero-precoverage limit. Curve c shows the sum of all carbon-containing desorption products (ethylene + EtOD + EtOH) as the water precoverage is increased; it follows the same general trend as observed for curve b. This shows that the amount of TEOS which dissociates (and later appears as ethylene and ethanol) increases $\sim 70\%$ as the water precoverage is increased. In addition, the product distribution, shown by the total ethanol/ethylene ratio in Figure 4, curve d, increases from a value of 1:1 at the extrapolated zero-precoverage water limit to a value of $\sim 3:1$ at the highest water precoverage. The 1:1 ratio with zero water indicates that the β -hydrogen elimination reaction (reaction 2 above) is the dominant decomposition pathway with no hydroxyls or water. This is also clear from the fact that

(33) Redhead, P. A. *Vacuum* 1962, 12, 203.

(34) Campbell, C. T.; Sun, Y.-K.; Weinberg, W. H. *Chem. Phys. Lett.* 1991, 179, 53.

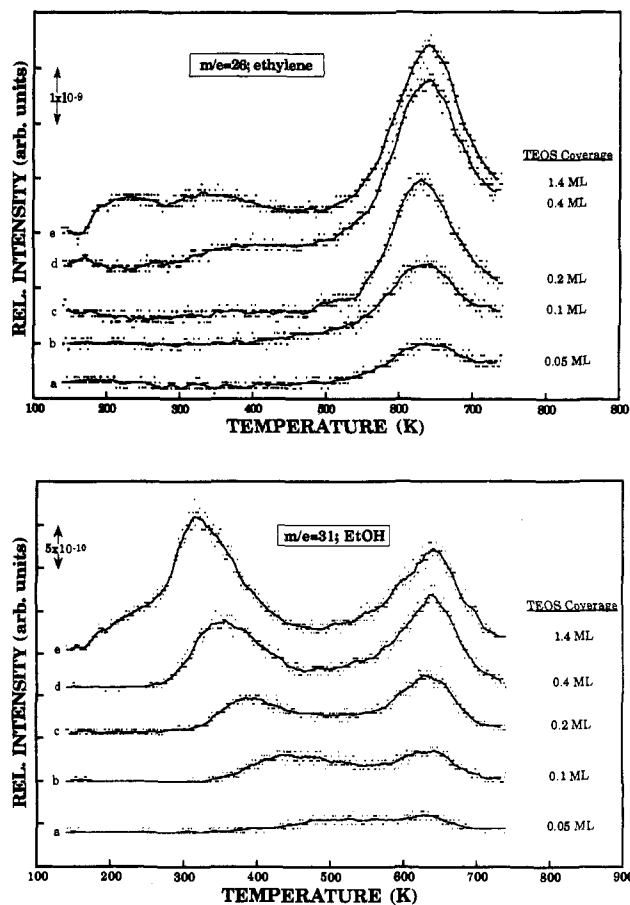


Figure 5. TPD spectra for (A) $m/e = 26$, ethylene, and (B) $m/e = 31$, EtOH, for varying TEOS exposures on TiO_2 . No D_2O pre-dose was given, but excess water accumulated in proportion to the TEOS dose. TEOS exposures were (a) 0.05 ML, (b) 0.13 ML, (c) 0.2 ML, (d) 0.4 ML, and (e) 1.4 ML. The arrows indicate QMS signals of 1×10^{-9} and 5×10^{-10} A, respectively.

the total EtOH + EtOD in the low-temperature peak extrapolates to zero at zero water. Since no carbon is left on the surface by 770 K (see below) and since one surface oxygen is left for every two ethoxy groups in reaction 2, we can conclude that a species of stoichiometry SiO_2 is left on the surface at 770 K following the decomposition of $\text{Si}(\text{OEt})_4$ according to this β -hydrogen elimination process.

TPD of TEOS on $\text{TiO}_2(110)$ with Excess Water. In another set of experiments, the TiO_2 crystal was exposed to increasing exposures of TEOS while excess H_2O was allowed to accumulate on the surface in proportion to the TEOS dose. The results are summarized in Figure 5 parts A and B, which show the $m/e = 26$ and $m/e = 31$ TPD curves, respectively. As expected, the desorption products show behavior similar to that of the high D_2O pre-doses in Figure 3A–E, with the exception that no deuterium-containing isotopes are present. The high-temperature desorption peak for $m/e = 26$, due to ethylene, increases with TEOS dose until reaching saturation at 0.4 monolayer coverage of TEOS. The additional features in the temperature range 150–450 K at $m/e = 26$ for higher TEOS exposures (Figure 5A, curve e) are due to the cracking pattern of desorbing TEOS and EtOH. The high-temperature desorption peak of ethanol at $m/e = 31$ behaves similarly to the high-temperature ethylene peak, as shown in Figure 5B. The low-temperature desorption peak of ethanol also varies with TEOS dose and saturates at a coverage of ~ 1 ML (not shown). Whereas a constant peak desorption temperature is observed for the low-temperature desorption peak of ethanol with increasing D_2O coverage (see Figure 3C–D), here the peak desorption temperature shifts to lower temperature with increasing TEOS dose. Its temperature is so high at very low

TEOS doses that the low- and high-temperature desorption peaks cannot be unambiguously resolved. Part of the intensity in the temperature range 350–550 K in Figure 5A and B may be due to desorption of a small quantity of diethyl ether, which has cracking fragments at $m/e = 31$ and 28.

The strongly decreasing TPD peak temperature of the low-temperature ethanol peak with increasing coverage, seen in Figure 5B, is indicative of a second-order rate-determining step according to simple Redhead analysis,³³ although more complex kinetics of a different order could also show this peak shift. For this set of experiments, the TEOS was dosed with a He carrier that contained H_2O impurity which was not trapped out. As a result, as the TEOS exposure was increased, the dose of water (which was present as an impurity in the TEOS) also increased proportionally. The subsequent second-order reaction



leading to ethanol desorption³¹ then accounts for the approximate second-order reaction kinetics observed in Figure 5B.

In contrast, increasing precoverages of D_2O and a constant, saturation TEOS dose lead to the first-order desorption characteristics (i.e., constant peak temperature³³) evident in the $m/e = 31$ and 32 TPD spectra of Figure 3C and D. There the He carrier gas was passed through a cold trap and the water contamination occurring during TEOS dosing was minimized. Thus, the concentration of only one reactant was increasing with exposure, and reaction (3) is expected to show pseudo-first-order kinetics, as observed.

XPS of TEOS on $\text{TiO}_2(110)$ with Excess Water. The XPS results reported here are for “excess” water doses large enough to ensure that the ethanol and ethylene TPD achieved their saturation line shapes (curve e in Figure 3A–E or the right-hand limit of Figure 4). A typical XPS experiment involved taking spectra of the clean surface, after dosing water and TEOS (~ 1.0 ML) to the surface and after brief flashes to 220, 440, and 770 K. These flash temperatures correspond to the removal of most of the molecularly desorbing TEOS and desorption of the low- and high-temperature decomposition peaks, respectively, observed in TPD.

Illustrated in Figure 6A are O(1s) data for this experimental series. Curve a is from the clean $\text{TiO}_2(110)$ surface, where lattice oxygen from the substrate has a BE of 529.9 eV. After TiO_2 is exposed to a coverage of ~ 1.0 ML of TEOS at 130 K, an additional feature in the O(1s) spectra appears at 532.8 eV, as illustrated in curve b. This binding energy is indicative of an oxygen atom bound in water- and alcohol-like environments.²⁶ Although not apparent in this figure, the peak area of the O(1s) signal decreases slightly with TEOS exposure due to attenuation of the substrate signal by the overlayer. (See Figure 7, below.) As shown in curve c, the shoulder at ~ 532.8 eV disappears when the sample is flashed to 220 K. This temperature is sufficiently high to remove most of the molecular TEOS (see Figure 1). Spectra taken of the O(1s) region after successive flashes to higher temperature are nearly identical to that shown in curve c, where the oxygen signal is primarily due to the metal oxide substrate. No change in the Ti($2p_{3/2}$) BE was detected throughout the deposition and reactions of TEOS on the surface, indicating that charge transfer to the depletion region and the resulting band bending were minimal.

Extensive reactions of TiO_2 with TEOS followed by high-temperature annealing in O_2 eventually caused small quantities of the adsorbed product SiO_2 to cluster into tall, three-dimensional islands or diffuse into the near bulk, leading to residual Si(2p) signals which could only be slowly removed by extended sputtering. The three-dimensional clustering of SiO_2 from TEOS reactions with TiO_2 powder has previously been reported.⁴ Small C(1s) signals from tantalum wires on the sample holder and not from the TiO_2 surface were also present in the XPS data. These features

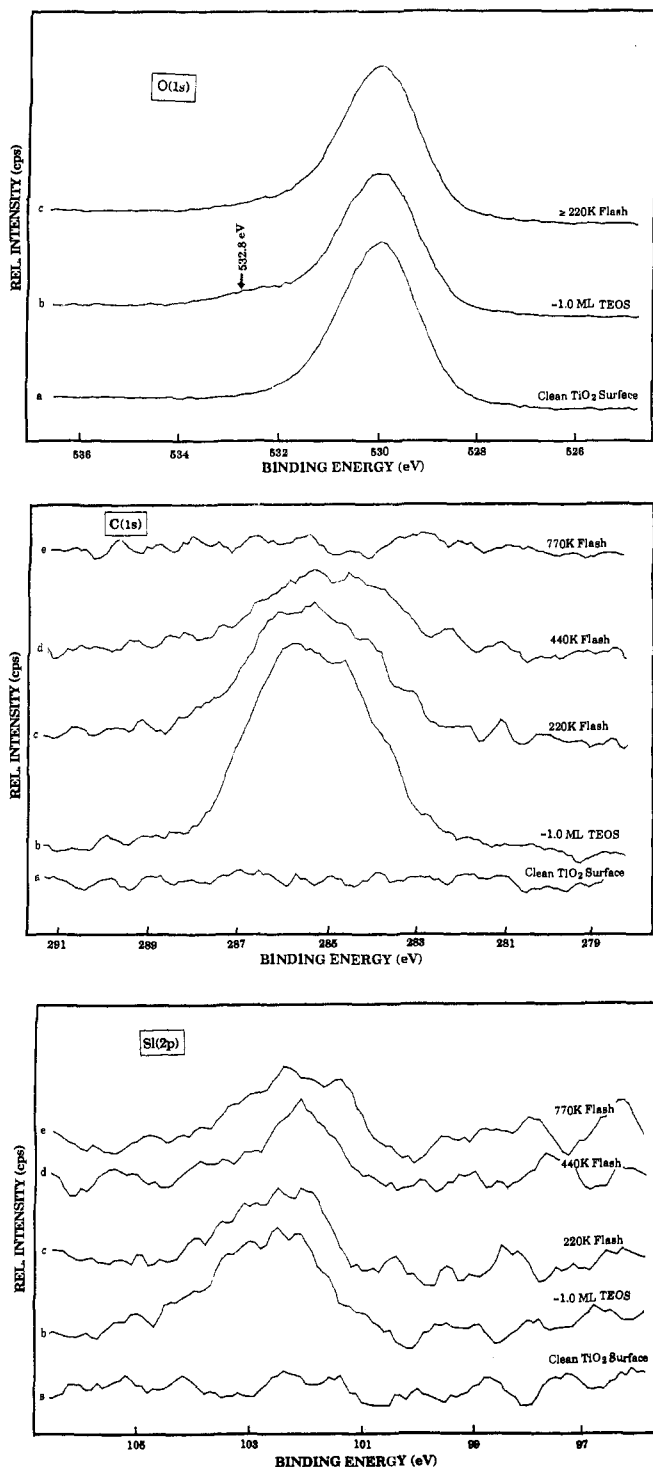


Figure 6. XPS spectra for (A) O(1s), (B) C(1s), (C) Si(2p) binding energy regions. TEOS was dosed to the $\text{TiO}_2(110)$ surface at ~ 130 K after excess water (~ 1.6 ML) was allowed to accumulate on the cold surface. The extent of the experiment is indicated as (a) clean $\text{TiO}_2(110)$ surface, (b) ~ 1.0 ML TEOS dosed at ~ 130 K, (c) 220 K flash, (d) 440 K flash, and (e) 770 K flash. Curve c in part A is representative of 220 K and successive flashes, as discussed in the text.

were always present in concentrations less than a few percent, and TPD spectra were independent of their presence, indicating that the reactions we are probing are inherent to the clean TiO_2 surface. To show the XPS features characteristic of TEOS on TiO_2 , we have subtracted these features from the spectra presented in Figure 6B and C.

Figure 6B illustrates the C(1s) region for the same set of experiments shown in Figure 6A. After dosing TEOS in the

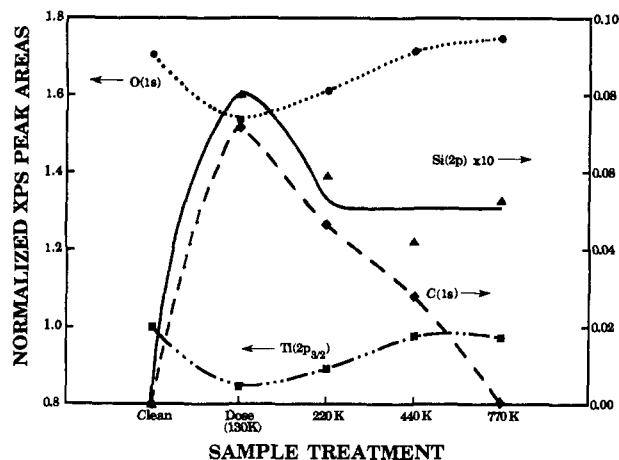


Figure 7. Normalized XPS peak areas versus extent of the experiment. All peak areas were normalized to the area of the clean $\text{Ti}(2p_{3/2})$ peak (1.0) prior to plotting. The O(1s) (●) and $\text{Ti}(2p_{3/2})$ (■) curves refer to the left axis, while the C(1s) (◆) and Si(2p) (▲) curves refer to the right axis.

presence of excess water, a peak appears that is centered about 285.5 eV (curve b). After flashing the sample to 220 K in order to remove most of the molecularly desorbing TEOS, the integrated C(1s) signal decreases by about 33% (curve c). As the sample is successively heated, this carbon signal is reduced again by about 36% after the 440 K flash (curve d). Finally, the C(1s) intensity decreases below the noise level after the 770 K flash (curve e).

Presented in Figure 6C is the corresponding Si(2p) region for the set of experiments just described. After dosing TEOS, a broad peak centered at ~ 102.6 eV appears, indicating adsorption of the alkoxysilane molecule (curve b). A decrease of about 33% in the integrated peak area is observed as the molecular layer is desorbed during the 220 K flash (curve c), consistent with Figure 6B. However, as indicated in Figure 6C, curves d and e, essentially no change is detected in the Si(2p) peak intensity within the error bars of its measurement ($\pm 15\%$) as the sample is successively flashed from 220 to 440 K and then to 770 K. The Si(2p) BE is ~ 102.2 eV after the flash to 770 K. This BE indicates that the remaining species, which has SiO_2 stoichiometry (see above), is built up from SiO_4 tetrahedra. (Bulk silicates have a BE of 102.6 eV, zeolites or aluminosilicates have 101.5-eV BE, and bulk silica has 103.0–103.5-eV BE.²⁶)

Figure 7 illustrates the behavior of these XPS peak areas, normalized to the clean $\text{Ti}(2p_{3/2})$, as a function of surface treatment and annealing. This annealing behavior is entirely consistent with that observed by TPD experiments. The C and Si signals increase after dosing TEOS and decrease after annealing to 220 K, due to some molecular desorption. All the carbon from TEOS is eventually removed from the surface: two molecules of ethanol (per TEOS molecule reacting) from the low-temperature decomposition peak, and one ethylene and one ethanol molecule from the high-temperature peaks. However, no Si is lost through this decomposition. On the basis of this discussion, we believe that a thin film of SiO_2 is formed on the $\text{TiO}_2(110)$ surface as a result of dosing TEOS and heating the sample to ~ 770 K. (The SiO_2 could also be in the form of three-dimensional islands less than ~ 20 Å thick, but thicker islanding would result in observable Si loss.)

To quantitate the absolute coverages of "1 ML" of adsorbed TEOS, we have analyzed relative XPS intensities using standard techniques.³⁵ The inelastic mean free paths³⁶ and surface atomic sensitivities³⁷ (in parenthesis) of the $\text{Ti}(2p_{3/2})$, C(1s), and Si(2p)

(35) Fadley, C. S. *Prog. Surf. Sci.* 1984, 16, 275.

(36) Seah, M. P.; Dench, W. A. *Surf. Interface Anal.* 1979, 1, 2.

transitions for our experimental conditions were taken from the literature values^{36,37} as 22 Å (1.2), 24 Å (0.25), and 25 Å (0.27), respectively. (The last four values were consistent with our measured C/Si intensity ratio from a TEOS multilayer.) In these calculations, we assume a uniform TEOS film whose density is the same as that in bulk, liquid TEOS (0.93 g/cm³). Following a ~1 ML TEOS dose at 130 K, a TEOS overlayer thickness value of 7.0 Å was determined from the C(1s)/Ti(2p_{3/2}) intensity ratio of ~0.08 (see Figure 7). Similarly, a thickness of 6.5 Å was determined from the Si(2p)/Ti(2p_{3/2}) intensity of ratio ~0.009 after this same dose.

Using the diameter of physisorbed TEOS determined from its bulk density (0.93 g/cm³) assuming close-packed spheres of TEOS (4.04 Å radius),³⁸ the thickness of a close-packed monolayer of TEOS is 6.6 Å. This value is within the error bars (~33% due to uncertainties in mean free paths) of the average value of 6.7 Å determined from the XPS results. Thus, the XPS results are consistent with such a spherical close-packing model, with 0.018 TEOS molecules per Å² at monolayer coverage or 0.35 TEOS molecules per TiO₂(110). (The TiO₂(110) unit cell has an area of 19.21 Å² and contains one unsaturated Ti⁴⁺ site and one unsaturated bridging oxygen.¹⁸) Following the flash to 220 K, which removes most of the molecularly adsorbed TEOS, the coverage is estimated to be 0.24 TEOS per TiO₂(110) unit cell on the basis of the fact that the C(1s) and Si(2p) peaks are decreased by ~31.5% after such a flash (see above). This is also consistent with the behavior of the Ti(2p_{3/2}) signal, which, following the flash to 220 K, recovers ~30% of the intensity lost during the TEOS dose.

The relative XPS intensities from the C(1s) and Si(2p) transitions were also used to estimate the stoichiometry of adsorbed species on the surface as a function of coverage and temperature. The C/Si atomic ratios after dosing and following the flashes to 220, 440, and 770 K were 8.0 ± 1, 7.8 ± 1, 4.6 ± 1, and 0 ± 1, respectively. (For these last three ratios, we used the Si(2p) area averaged between the 220, 440, and 770 K values, since it stayed relatively constant in this temperature range and since no Si was removed from the surface according to TPD.)

Examination of the TiO₂ crystal after the 770 K flash by LEED showed only the p(1 × 1) spots of the substrate, indicating a disordered overlayer structure. In a separate experiment, LEED observations were made of this same type of overlayer after flashes to 300, 440, and 770 K, and no ordered overlayers were observed (i.e., only the p(1 × 1) spots were seen).

Further evidence that the surface SiO₂ species remaining after heating TEOS adlayers to 770 K was made up of SiO₄ tetrahedra was provided by XPS experiments where more concentrated SiO₂ layers were built by repeating ten dose/flash cycles to 770 K. The Si(2p) peak area after this was ~3 times that after the first cycle (the top curve in Figure 6C), but it had nearly the same binding energy (102.2 eV), characteristic of the SiO₄ tetrahedra in silica and silicates (101.5–103.5 eV).²⁶ In these cycles, the TPD spectrum was also monitored, and the amounts of desorbing ethanol and ethylene decreased by ~30% with each cycle. The molecular desorption of TEOS correspondingly increased. This indicates that the SiO₂ layer is covering the TiO₂ and thereby masking sites needed for reaction with TEOS. This intimate contact with the Ti⁴⁺ cations might explain why this Si(2p) BE is somewhat higher here than in bulk silica itself (103.0–103.5 eV²⁶). Surface core level shifts might also play a role here.

Discussion

When TEOS is exposed to a water-free TiO₂(110) surface held at 130 K, it adsorbs intact with a sticking probability near unity. At high exposures, both multilayers and a molecularly

adsorbed TEOS layer are formed. Upon heating this surface, the multilayer desorbs in a sharp, zero-order peak whose peak temperature is 185 K. The molecular peak is more strongly bound to the substrate and does not desorb until ~230 K. Quantitative XPS with excess water suggests that, upon annealing the surface to 220 K, ~32% of the chemisorbed TEOS desorbs in this molecular peak. The remaining 68% of the TEOS ML dissociates somewhere between 130 and 300 K. In the absence of water, dissociation of the chemisorbed TEOS also occurs below 300 K, but now only about half as much (34% of a ML) dissociates (Figure 4), and more desorbs (Figure 3A). The amount that dissociates (34% of a ML, or 0.12 per unit cell) exceeds the defect concentration on this surface, which is thought to be below 3%.¹⁷

Silicon alkoxides are known to undergo hydrolysis reactions leading to cleavage of the Si–O bond,^{2–4} and it has generally been thought that the presence of surface MOH groups (M = metal) were necessary to form M–O–Si bonds in alkoxy silane coupling to metal oxides.¹ However recent reports indicate that dissociative adsorption of silicon alkoxides can occur at 200 K on the Lewis base sites of MgO(100)¹³ and at 300 K on strained siloxane defects of dehydroxylated silica, in the absence of surface OH.^{14,15} Our data indicate TEOS couples to normal (nondefect) sites on the TiO₂(110) surface, thus forming Ti–O–Si bonds, with a high rate at 300 K even in the *absence* of surface water or hydroxyl groups. Since TiO₂ is generally considered weakly acidic and MgO is basic, perhaps this coupling mechanism is rather general.

The mechanism for this coupling reaction is probably a surface-induced, nucleophilic substitution reaction. In basic media, alkoxy silanes are known to undergo nucleophilic substitution leading to cleavage of an Si–O bond.³⁹ Although TiO₂ is generally considered a weakly acidic oxide, bridging oxygens (like those on this TiO₂(110) surface) are Lewis base sites.⁴⁰ In the absence of water or adsorbed hydroxyls, these are likely nucleophiles for the attack of adsorbed TEOS, leading to cleavage of an Si–OEt bond, while forming a new TiO–Si bond between the Si atom and bridging oxygen from the TiO₂. The displaced EtO binds to the nearby Ti⁴⁺ site, and in fact a simultaneous electrophilic attack by this Ti⁴⁺ may assist the nucleophilic attack. On a defect-free (bulk-terminated) TiO₂(110) surface, these Ti⁴⁺ sites are five-coordinate (versus six-coordinate in the bulk) and can therefore easily accommodate this OEt ligand. The dissociation reaction is shown schematically as the first step in the proposed reaction mechanism presented below (reaction 4).

The XPS data following desorption of the molecular layer is consistent with this mechanism. Following desorption of the molecular TEOS layer during the anneal to 220 K, the C(1s) line shape from the remaining surface species is consistent with the dominant presence of EtO groups. The C(1s) spectra as dosed and after the 220 K flash were well fitted with two equal-area Gaussian peaks of fwhm = 1.7 eV (instrument resolution) separated by 1.4 eV, which is the known separation in BE from the two inequivalent carbons in ethoxy-like species.^{31,41} In addition, the C/Si atomic ratio of ~8 indicates that all carbon remains on the surface following dissociation of the TEOS molecule. Adsorbed EtO groups have been observed previously in this temperature range after reaction of EtOH with TiO₂(110) facets.³¹ We cannot tell from our data whether one or two ethoxy groups are cleaved from Si during the dissociation process in the absence of water. Both adsorbed triethoxysilyl and diethoxysilyl species are feasible products, the former being bound to a single bridging oxygen and the latter being bound to two adjacent bridging oxygens. Mixtures of both species have been reported for TEOS reacting with SiO₂.¹²

(39) Pawlenko, S. *Organosilicon Chemistry*; Walter de Gruyter: New York, 1986; p 6.

(40) Tanabe, K.; Misono, M.; Ono, Y.; Hattori, H. *New Solid Acids and Bases: Their Catalytic Properties*; Elsevier: New York, 1989.

(41) Bomben, K. D.; Jolly, W. L. *J. Electrom Spectrosc. Relat. Phenom.* 1980, 20, 333.

(37) Wagner, C. D.; Davis, L. E.; Zeller, M. V.; Taylor, J. A.; Raymond, R. H.; Gale, L. H. *SIA. Surface Interface Analysis* 1981, 3, 211.

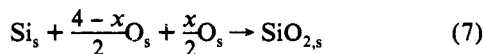
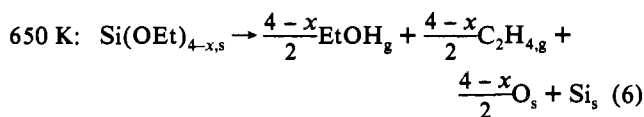
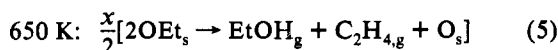
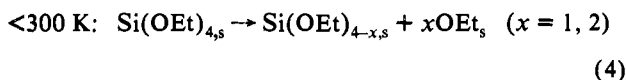
(38) Campbell, C. T. *Surf. Sci.* 1986, 167, L181.

In the absence of surface water (or hydroxyls), the EtO and Si(OEt)_{4-x} dissociation products are thermally stable to ~650 K, where they both decompose via β -hydrogen elimination reactions to yield equal parts of EtOH and ethylene gas; an SiO₂ surface species made up from SiO₄ tetrahedra is also produced. This reaction mechanism is consistent with the C(1s) peak areas which show that all carbon is removed from the surface after annealing to 770 K, and the TPD spectra, which indicate that ethylene and EtOH are the predominant desorbed products from the high-temperature peak, appearing in a one-to-one ratio. In addition, no significant quantities of acetaldehyde or other dehydrogenation products, which would be expected from α -elimination reactions, are observed.

In the absence of D₂O, we cannot distinguish from our data whether the EtO groups are attached to Ti or Si atoms, or both, at the time of β -hydrogen elimination (~650 K), but it is clear from the TPD that all ethoxide groups decompose at about the same temperature (i.e., with about the same activation energy). The activation energy for the β -hydrogen elimination reaction can again be estimated from Redhead analysis³³ of the peak temperature in the TPD spectra. Assuming a preexponential factor of 10¹¹ s⁻¹ for a rate determining step involving intrasorbate bond breaking,³⁴ the activation energy at $T_p = 650$ K (reactions 6 and 18 below) is 34.4 ± 0.5 kcal/mol. The activation energy for β -hydrogen elimination at an EtO group is probably insensitive to whether the third nearest neighbor is Si or Ti. After hydrogen is eliminated from one EtO group, leaving oxygen and evolving ethylene, the H must rapidly migrate to a neighboring EtO, where it reacts to form EtOH, which then desorbs simultaneously with ethylene.

From the Si(2p) XPS results it is apparent that, after desorption of molecular TEOS (220 K anneal), no further silicon-containing species are desorbed at higher temperature (see Figures 6C and 7). Rather, SiO₂ species remain on the surface following the β -hydrogen elimination reactions.

Consistent with the observations discussed above, we propose the following reaction sequence to explain the interaction of TEOS with a TiO₂(110) surface in the absence of adsorbed water.

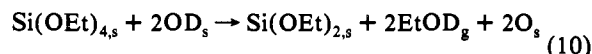


Reaction 7 may not be needed here since the Si-O bonds may already be established in prior steps. We cannot tell from the present data, so we purposefully leave these species ill-defined.)

In the presence of surface D₂O (or HDO, H₂O), somewhat different behavior was observed. First, more TEOS dissociated. This was apparent both from the decrease in the amount of molecular TEOS desorbed (Figure 3A) and from the increase of TEOS dissociation products observed in TPD as a function of predosed D₂O (Figure 4). Second, half of the surface C is already removed as EtOD (+EtOH) by 350 K in the presence of excess water (see Figures 4 and 7). Thus, TPD intensities (Figure 4) give the following net stoichiometry for this low-temperature TEOS dissociation reaction:



and

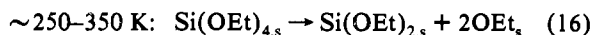
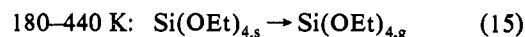
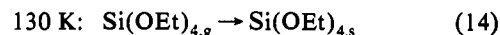
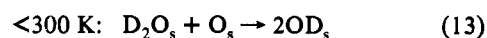
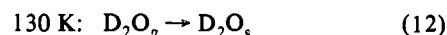


It is thus clear that two of the EtO groups (per reacting TEOS) are more reactive with surface hydroxyls, since they come off the surface as EtOD (+EtOH) at 350 K in the presence of excess water (see Figure 4). Since Ti-bound EtO groups on TiO₂(110) are known to react with OH_s at ~350 K to give EtOH gas,³¹ these more reactive EtO groups are assumed to be bound to the TiO₂ surface. We therefore postulate that the two remaining EtO groups are still bonded to Si after this 350 K peak completes. The 1:1 ratio of EtOH/C₂H₄ in the high-temperature peak (Figure 4) is clearly consistent with the reaction

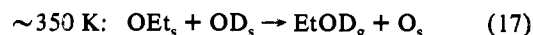


which is nearly the same as reaction 2 and step 6 above. Again, this is initiated by β -hydrogen elimination on an ethoxy group at 650 K, as in the absence of D₂O predose. Together, these net reactions give the proper 3:1 total ratio of EtOH + EtOD/C₂H₄ (Figure 4).

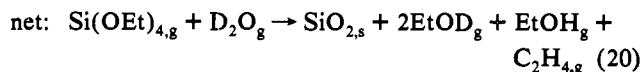
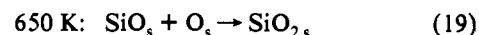
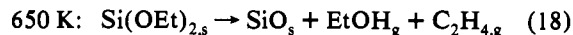
A full reaction mechanism which would be consistent with these observations in the presence of excess D₂O is then



(This may occur as a two-step process via Si(OEt)_{3,s}.)



(This reaction occurs twice for every reacting TEOS.)



(In reaction 20, we omit the desorption of TEOS.)

Previously observed reactions on TiO₂ are used in many of these steps (reactions 12,^{17,18} 13,^{17,18} and 17³¹), and they occur here at the previously observed temperatures.^{17,18,31} The combination of reaction steps 12, 13, 15, 16, and 17 is essentially the hydrolysis of TEOS by water to form Si(OEt)_{2,s}, O_s, and two ethanol molecules. Water is known to hydrolyze silicon alkoxides to form an alcohol and an alkoxysilyl fragment at room temperature.²⁻⁴ New in our present results is the observation that the water or hydroxyls are needed only to eliminate the surface EtO, but that the coupling of the silane to the TiO₂ occurs readily without water or hydroxyls.

Further evidence for the diethoxysilyl surface species proposed here was obtained by dosing TEOS to the TiO₂ surface at 130 K in the presence of excess water (D₂O) and then heating to 440 K. Desorption of ethanol was observed from the low-temperature peak as described above. The sample was then cooled to 130 K and dosed again with multilayer water (D₂O). Upon heating again, no further desorption of low-temperature ethanol (EtOD) was observed at 350 K, and the amount of high-temperature ethylene and EtOH evolved at 650 K was not reduced by this intermediate D₂O dose. If any adsorbed EtO species had remained on TiO₂ sites after the initial 440 K flash, they would have reacted readily with hydroxyls in the subsequent flash to give a 350 K EtOD peak³¹ and the amount of high-temperature ethanol + ethylene would have been reduced. Thus, the stoichiometries in

Figure 4 truly reflect mechanisms and are not controlled by competing kinetics. Of course, water or hydroxyls may (and indeed probably do) also react with this diethoxysilyl species, but the rate is too slow to be seen within a single surface residence time probed by such ultra-high-vacuum experiments.

In the case of "excess-water" experiments, the intermediate of stoichiometry $\text{Si}(\text{OEt})_{2,x}$ is thus well established by the TPD and XPS intensities and by the lack of reactivity of this species with further water. The simplest explanation, and the one we will adopt here, is that this same intermediate is also formed in the absence of water. Thus, we propose that $x = 2$ in reactions 4–7, such that reaction 4 is equivalent to reaction 16, reactions 6 and 18 are the same, and reactions 7 and 19 are the same.

Inherent to our proposed mechanism is an explanation for the increasing amount of TEOS dissociation with water pre-dose. Since water facilitates the removal of surface OEt from Ti sites, via reaction step 17 above, it creates new free sites needed in step 16 for TEOS dissociation. In the absence of sufficient free sites, some of the TEOS instead desorbs at high coverage. The high-temperature part of the molecular desorption peak for TEOS is suppressed by water addition for the same reason: more of the TEOS dissociates.

Conclusion

We have exposed a $\text{TiO}_2(110)$ single-crystal surface to TEOS at low temperatures, ~ 130 K. In some cases, the crystal surface was nearly void of water and hydroxyls, while, in others, the surface was pretreated with D_2O . In either case, a disordered SiO_2 overlayer, made from SiO_4 tetrahedra, was produced with high probability upon heating to 750 K, as evidenced by XPS,

TPD, and LEED. For the water-free surface, TPD and XPS show the net dissociation and reaction products after heating to 770 K to be two ethanol and two ethylene molecules and a surface SiO_2 unit per reacted TEOS molecule. All of these products are observed in a high-temperature desorption peak, centered at ~ 650 K, rate-limited by β -hydrogen elimination at ethoxy groups. When excess water is present on the surface, ethanol production and TEOS dissociation is enhanced, yielding a surface-bound diethoxysilyl group. This $\text{Si}(\text{OEt})_{2,x}$ species binds to the surface via two Ti–O–Si bonds. It is produced by 350 K in abundance exceeding the surface defect concentration, even when no surface hydroxyls or water are present with the TEOS. The amount of TEOS dissociating to produce this species (and eventually surface SiO_2) increases with increasing water coverage up to a limit of about twice that in the no water case, or 68% of a ML. In excess water, the net TPD products are two ethanol molecules in a low-temperature peak (350 K) and a high-temperature desorption peak (650 K) consisting, again, of one ethanol and one ethylene molecule (per molecule of dissociated TEOS).

Acknowledgment. The authors gratefully acknowledge the support for this work by the Department of Energy, Office of Basic Energy Sciences, Chemical Science Division, and the National Science Foundation (C.T.C.) and Pacific Northwest Laboratories (J.W.R.). J.W.R. also wishes to acknowledge helpful discussions with B. Bunker and B. D. Kay of PNL. C.T.C. wishes to thank M. A. Barteau, J. Crowell, and L. H. Dubois for helpful discussions and acknowledges the Camille and Henry Dreyfus Foundation for a Teacher–Scholar Award.